ISSN 0001-4338, Izvestiya, Atmospheric and Oceanic Physics, 2014, Vol. 50, No. 6, pp. 630–637. © Pleiades Publishing, Ltd., 2014.
Original Russian Text © T.G. Talipova, E.N. Pelinovsky, A.A. Kurkin, O.E. Kurkina, 2014, published in Izvestiya AN. Fizika Atmosfery i Okeana, 2014, Vol. 50, No. 6, pp. 714–722.

Modeling the Dynamics of Intense Internal Waves on the Shelf

T. G. Talipova[a, b], E. N. Pelinovsky[a, b], A. A. Kurkin[a], and O. E. Kurkina[a, c]

[a] *Nizhnii Novgorod State Technical University, ul. Minina 24, Nizhnii Novgorod, 603950 Russia*
[b] *Institute of Applied Physics, Russian Academy of Sciences, ul. Ul'yanova 46, Nizhnii Novgorod, 603950 Russia*
[c] *National Research University, High Economic School, ul. Myasnitskaya 20, Moscow, 101000 Russia*
e-mail: tgtalipova@mail.ru

Received September 6, 2013

Abstract—The transformation of the internal wave packet during its propagation over the shelf of Portugal was studied in the international experiment EU MAST II MORENA in 1994. This paper presents the results of modeling of the dynamics of this packet under hydrological conditions along the pathway of its propagation. The modeling was performed on the basis of the generalized Gardner–Ostrovskii equation, including inhomogeneous hydrological conditions, rotation of the Earth, and dissipation in the bottom boundary layer. We also discuss the results of the comparison of the observed and simulated forms and phases of individual waves in a packet at reference points.

Keywords: internal waves, transformation, Gardner equation, shelf of Portugal

DOI: 10.1134/S0001433814060164

INTRODUCTION

Modeling of the generation and propagation of internal waves and their transformation on the ocean media irregularities is currently in demand in relation to the development of shelf regions in seas and oceans. Physicomathematical models of several levels have been developed. Analytical linear models were historically the first to be elaborated [1]. Then, nonlinear models appeared that were developed with the application of the asymptotic methods in the approximation of low nonlinearity and small dispersion [1–3]. The Korteweg–de Vries equation should be emphasized among these approximate models of internal waves as a model of the first level of nonlinearity [3, 4]. Models of the second level include generalizations of the Korteweg–de Vries equation of higher nonlinearity and dispersion levels for a horizontally nonuniform rotating ocean with account for energy losses [5, 6]. These models were frequently applied in the approximation of two layer stratification [7–9], but it is not difficult to numerically calculate the equation parameters for continuous stratification as well [5, 6]. The models of the second level include the models developed on the basis of the Camassa–Choi system [10]. They include full nonlinearity and low dispersion. These models were developed for waves in a two-layer ocean. By the present time, models of the higher third level have been developed based on the Euler or Navier–Stokes equations of full nonlinearity, which also take into account the bottom topography and rotation of the earth [11–13]. However, so far these models do not allow the existence of relatively stable background horizontally nonuniform stratification, which is characteristic of real oceanic conditions and well realized in the approximate models. The application of the approximate models of the second level is useful also because it makes it possible to analytically predict one or another peculiarity of the dynamics of internal waves at a relatively low number (from four to six) of parameters, which cannot be revealed in the equations of full nonlinearity. For example, the authors of this paper used an approximate model of the second level (the Gardner equation) to predict the existence of quasi-stationary trains of long internal waves, so-called breathers, the dynamics of which was later demonstrated in a model of full nonlinearity [14].

An approximate model of the second level developed by the authors on the basis of the Gardner–Ostrovskii equation was applied to describe the field of internal waves over the northwestern shelf of Australia [5, 6, 15, 16], in the Arctic [15–17], and on the Malin shelf [15, 16, 18]. Modeling of the dynamics of internal waves was carried out in [18] as the wave train propagated over the Malin shelf. The form of the wave train was compared with the data of observations recorded at reference points of the train propagation. A similar experiment was also conducted on the shelf of Portugal [19–21]. In this work, we model the dynamics of this wave train and compare the results of modeling with the observations of internal waves at reference points.

2. THEORETICAL MODEL

The Gardner–Ostrovskii equation is well known as a model to describe the dynamics of long internal waves in a horizontally homogeneous ocean. The model also allows us to take into account the rotation of the earth. The main equation of this model is written as [6, 22, 23]

$$\frac{\partial \varsigma}{\partial x} + \left(\frac{\alpha Q}{c^2}\varsigma + \frac{\alpha_1 Q^2}{c^2}\varsigma^2\right)\frac{\partial \varsigma}{\partial s} + \frac{\beta}{c^4}\frac{\partial^3 \varsigma}{\partial s^3} + \frac{kcQ}{\beta}\varsigma|\varsigma| = \frac{f^2}{2c}\int \varsigma ds, \tag{1}$$

where

$$\varsigma(x,s) = \frac{\eta(x,t)}{Q(x)} \text{ and } Q = \sqrt{\frac{c_0^3}{c^3}\frac{\int (d\Phi_0/dz)^2 dz}{\int (d\Phi/dz)^2 dz}} \tag{2}$$

(index "0" denotes the values corresponding to the first reference station with coordinate x_0). Hereinafter we use the Boussinesq approximation. Variable s is "slow" time in the accompanying coordinate system

$$s = \int \frac{dx}{c(x)} - t. \tag{3}$$

Variable s is the isopycnals displacement at the maximum of the mode function, which is found from the solution of the Sturm–Liouville problem,

$$\frac{d^2\Phi}{dz^2} + \frac{N^2(z)}{c^2}\Phi = 0, \tag{4}$$

with zero boundary conditions at the bottom and surface (rigid lid approximation):

$$\Phi(0) = \Phi(H) = 0, \tag{5}$$

It is normalized as follows

$$\Phi_{\max} = 1, \tag{6}$$

where H is the basin depth; velocity c is also found from (3)–(4). It is the linear velocity of the propagation of long internal wave of the corresponding mode, and coefficients of dispersion β, quadratic nonlinearity α, and cubic nonlinearity α_1 are calculated in quadratures from mode function Φ and its derivatives (see [17, 24])

$$\beta = \frac{c}{2}\frac{\int \Phi^2 dz}{\int (d\Phi/dz)^2 dz}, \tag{7}$$

$$\alpha = \frac{3c}{2}\frac{\int (d\Phi/dz)^3 dz}{\int (d\Phi/dz)^2 dz}, \tag{8}$$

$$\alpha_1 = -\frac{\alpha^2}{c} + 3c\frac{\int\left[(d\Phi/dz)^4 - (N^4\Phi^4/c)^4\right]dz}{\int (d\Phi/dz)^2 dz} + 3c \times \frac{\int\left[c(d\Phi/dz)^2 + (N^2\Phi^2/c) - (2\alpha/3)(d\Phi/dz)\right](dT/dz)dz}{\int (d\Phi/dz)^2 dz}, \tag{9}$$

where $T(z)$ is a nonlinear correction to the mode, which is found from the solution of the following equation

$$\frac{d^2T}{dz^2} + \frac{N^2}{c^2}T = \frac{\alpha N^2}{c^4}\Phi + \frac{\frac{d}{dz}(N^2)}{c^3}\Phi^2 \tag{10}$$

with zero boundary conditions at the bottom and water surface

$$T(0) = T(H) = 0 \tag{11}$$

It is normalized as

$$T(z_{\max}) = 0. \tag{12}$$

The rotation of the earth is taken into account through the Coriolis parameter, where $T_c = 24$ h and φ is the geographical latitude. Finally, the model includes a dissipation term, which allows us to take into account the friction in the bottom turbulent boundary layer [5]; k is the friction coefficient, which is selected phenomenologically.

Equation (1) is solved with the periodical boundary conditions with respect to time

$$\varsigma\left(s + \frac{2\pi}{\omega}, x\right) = \varsigma(s,x) \tag{13}$$

and initial conditions

$$\varsigma(s,x_0) = \eta(s,x_0). \tag{14}$$

Equation (1) conserves the zero mass

$$\int \varsigma(s,x)ds = 0 \tag{15}$$

and energy flux

$$\int \varsigma^2(s,x)ds = a_0^2 \int F^2(s)ds \tag{16}$$

if dissipation is zero.

3. DATA OF OBSERVATIONS AND THEIR PROCESSING FOR MODELING

The data of observations of the internal wave train transformation were obtained in the course of the European field experiment EU MAST II MORENA in 1994 on the shelf of Portugal [19–21]. The data were given to the authors by T. Sherwin within the joint grant INTAS-RFBR no. 95969. The measurements were carried out in August 1994 on the shelf of Portugal at three points, which in the course of the experi-

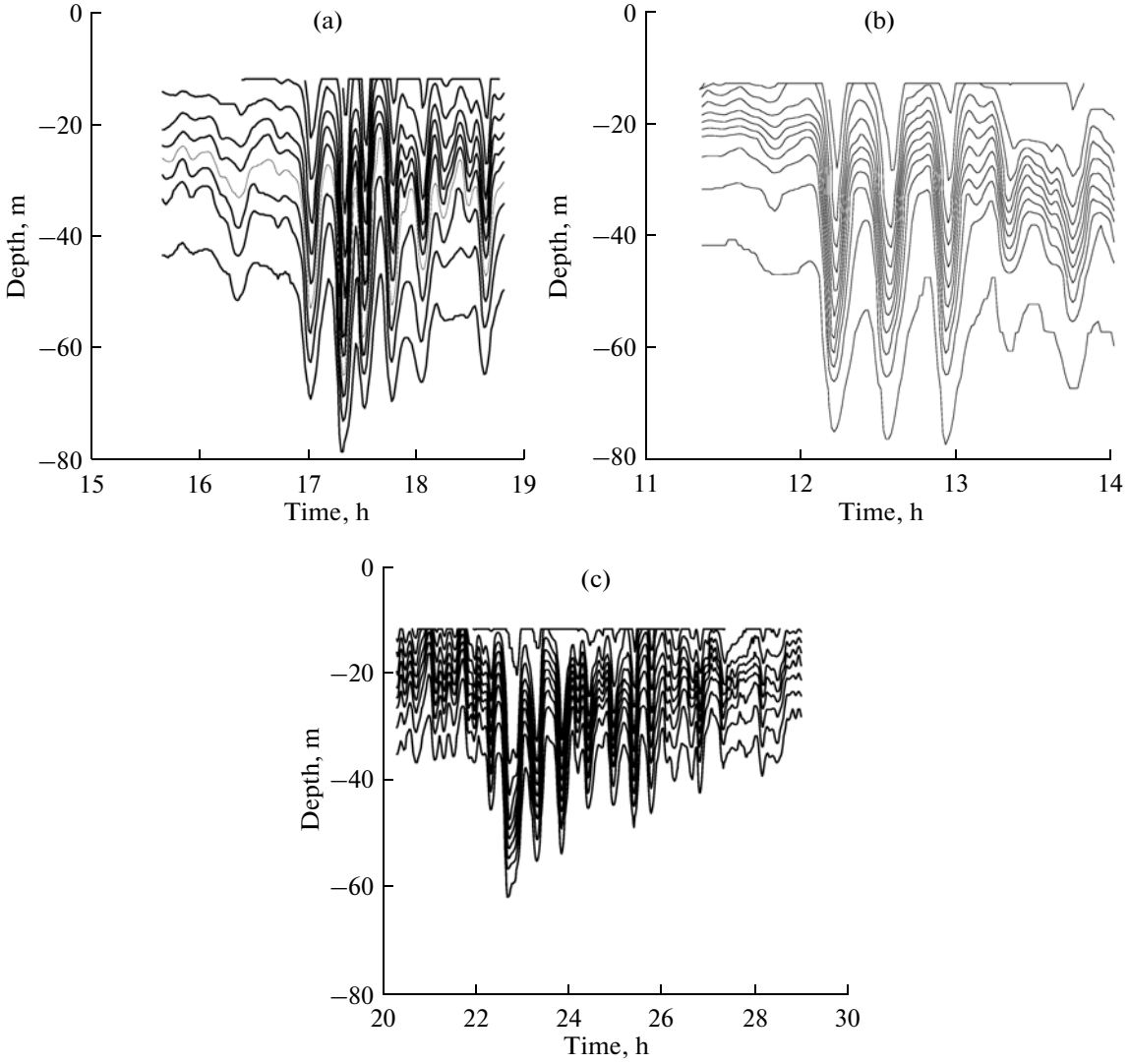

Fig. 1. Displacements of isotherms at points (a) 14, (b) 15, and (c) 16. The lower isotherm corresponds to a temperature of 13.5°; the temperature difference between isotherms is 0.5°.

ment were numbered as 14, 15, and 16. Their coordinates are given in Table 1.

All the points are located along a straight line; the distance between points 14 and 16 is 26.3 km. The measured profile of the wave train at point 14 is the input one for numerical modeling. Displacements of isotherms calculated from the temperature measurements are shown in Fig. 1 for all three points.

Table 1. Coordinates of the stations

Number of the point	Latitude	Longitude
14	41°03′	9°15.8′
15	41°04.8′	9°08.4′
16	41°06.5′	9°01.7′

An analysis of the modal structure based on the available records of internal waves demonstrated that the first mode dominates in the records with a proportion of 95%. The initial wave profile at point 14 consists of three solitonlike waves whose number increases as the wave train transforms (Fig. 1).

The mode function and coefficients of Eq. (1) are calculated on the basis of unperturbed (mean) vertical profile of the Brunt–Väisälä frequency, which is shown in Fig. 2 for each point.

The coefficients of the model are calculated from formulas (2)–(4), (5)–(10), and (12); they are presented in Table 2. All coefficients notably change along the pathway of the wave.

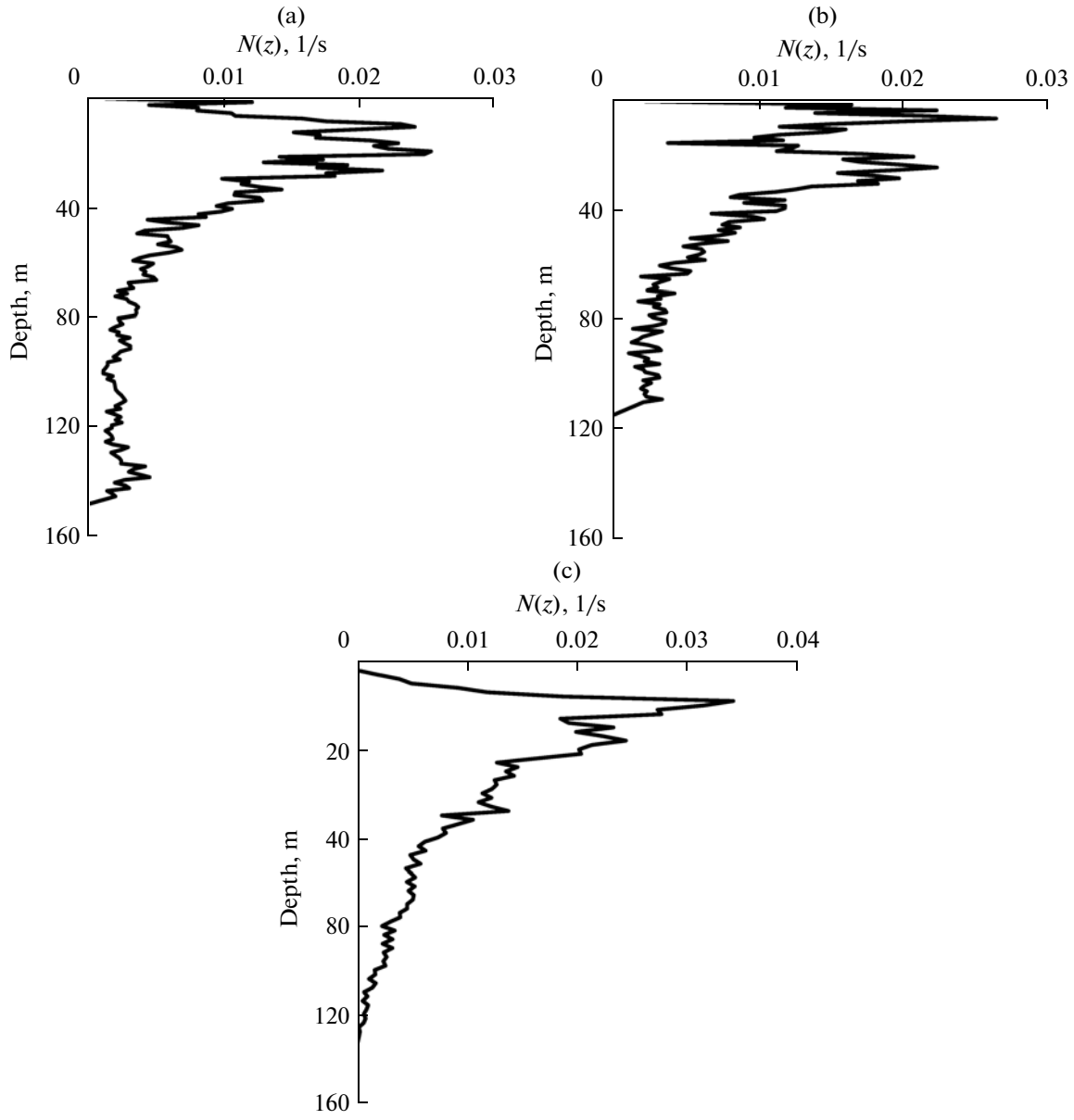

Fig. 2. Mean profile of the Brunt–Väisälä frequency at points (a) 14, (b) 15, and (c) 16.

The Gardner–Ostrovskii equation (1) for the modeling wave transformation during its propagation along the horizontally inhomogeneous pathway is written for the vertical displacement of isopycnals $\eta(x, t)$ at the maximum of the first mode. Knowing the observed displacements of isotherms (Fig. 1) and assuming that all oscillations occur in the first mode, we calculate the displacement function at the maximum of the first mode from each isotherm

$$\eta(x,t) = \frac{\xi(z,x,t)}{\Phi(z)}, \tag{17}$$

Table 2. Coefficients of the model

Number of the poin	Distance, m	Depth, m	α, s^{-1}	β, m^3/s	c, m/s	α_1, $m^{-1}\,s^{-1}$	Q
14	0.0	153	−2.39E-02	297.7	4.57E-01	−8.73E-04	1
15	13590	131	−2.47E-02	341.6	5.65E-01	−2.41E-04	0.95
16	26280	93	−1.81E-02	123.6	3.75E-01	−7.57E-04	1.26

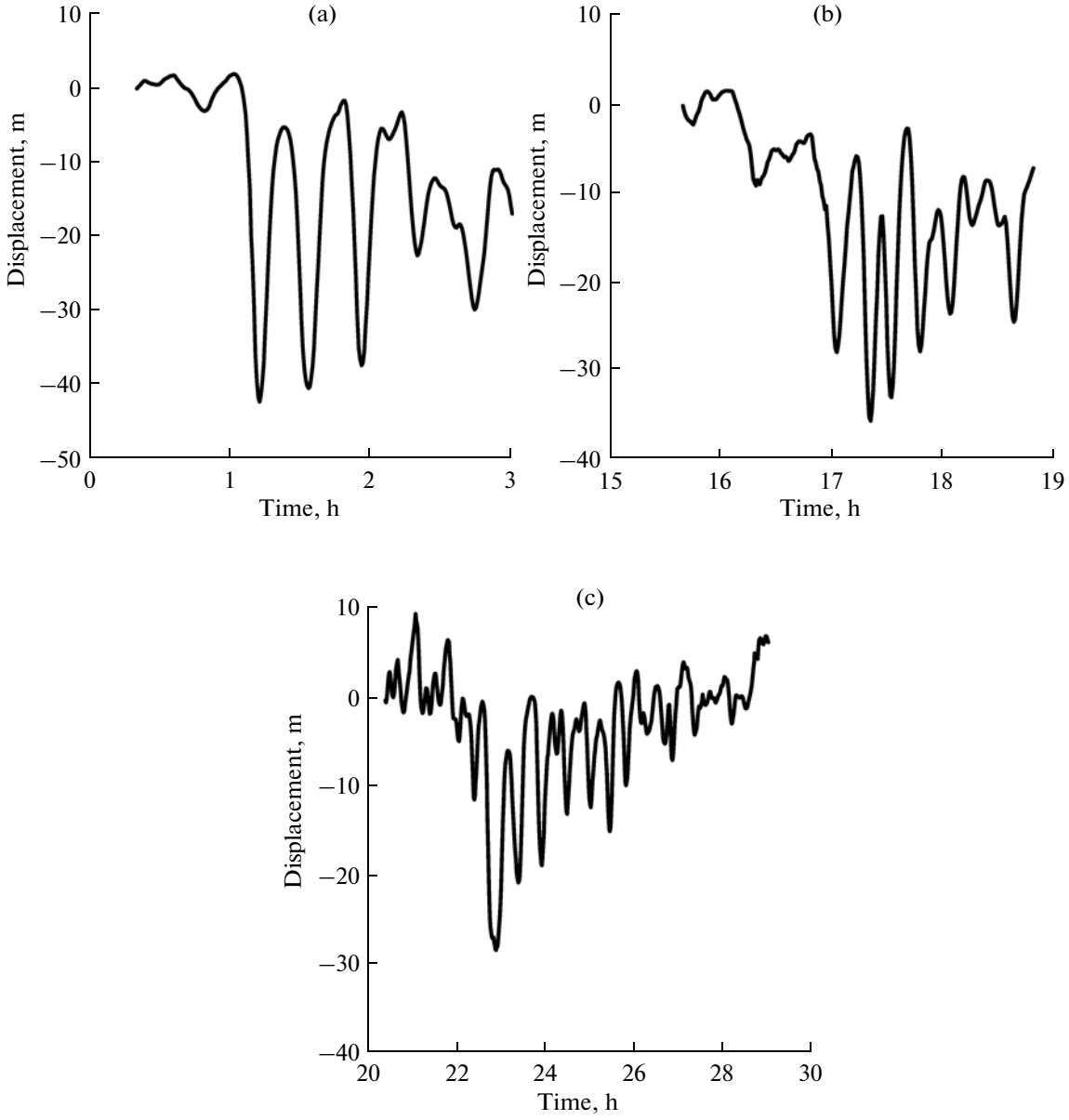

Fig. 3. Wave profiles at points (a) 14, (b) 15, and (c) 16.

where $\Phi(z)$ denotes the mode function and $\xi(z, x, t)$ are observed displacements of isotherms. As a rule, the forms of the isotherm displacements calculated from relation (21) at the maximum of the first mode $\eta(x, t)$ do not completely coincide with each other and we use the averaging procedure. We already used this method in [18]. The results of calculations of the wave profile from the data of observations at each point are shown in Fig. 3. The zero level corresponds to the location of the first mode maximum at each point.

The wave profile at point 14 is taken as the initial data for the numerical modeling of Eq. (1).

4. RESULTS OF NUMERICAL MODELING

It was mentioned above that periodical boundary conditions in time were used in the modeling. Taking into account the fact that internal waves on the shelf are generated mainly by the semidiurnal barotropic tide (with a period of 12.4 h), the time series of internal wave at point 14 was supplemented by a nonperturbed time series so as to obtain a period coinciding with the period of the semidiurnal tide. This record became the initial one for the model. We note that the differential scheme of the numerical solution of the Gardner–Ostrovskii equation (1) and its stability was discussed

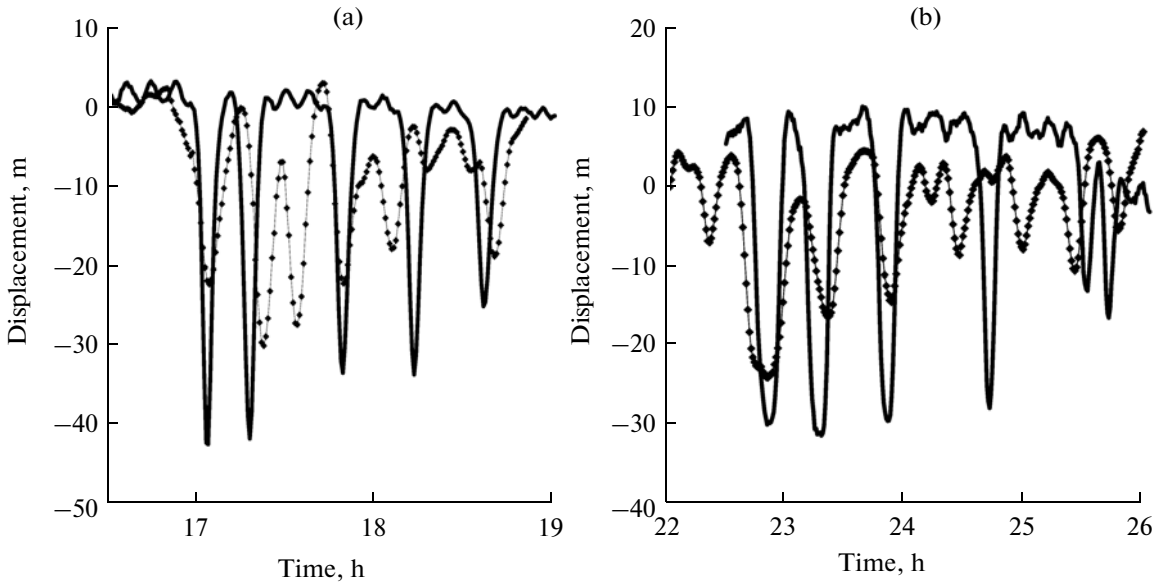

Fig. 4. Comparison of the modeling results (solid line) with the data of observations (dots) at points (a) 15 and (b) 16 in the absence of bottom friction.

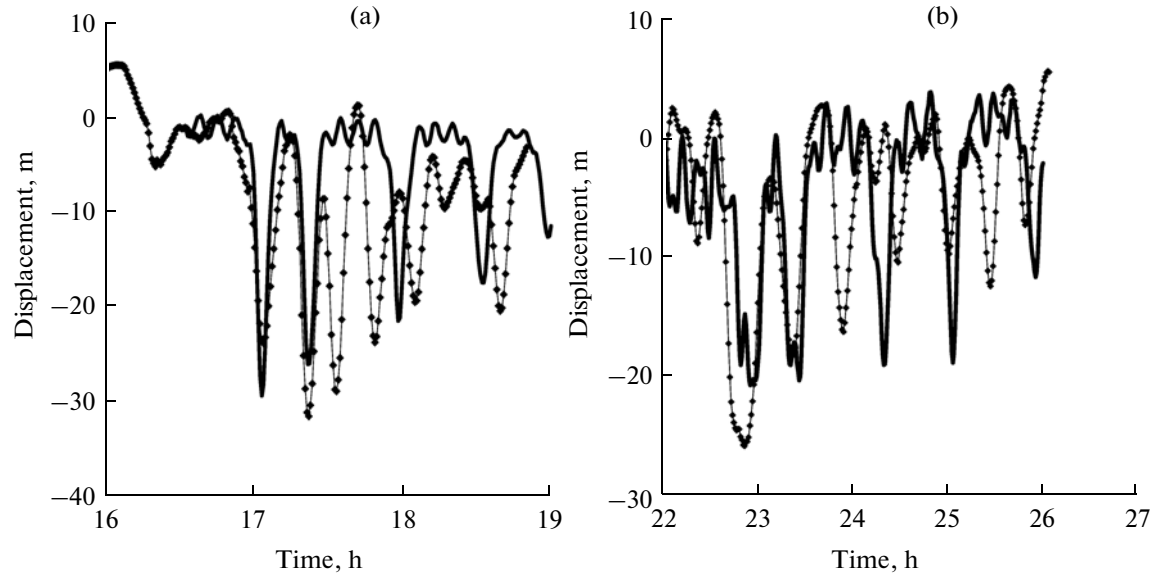

Fig. 5. Comparison of the modeling results (solid line) with the data of observations (dots) at points (a) 15 and (b) 16 when the coefficient of bottom friction is 0.0006.

in [5, 6, 25]. We used the same numerical scheme in our work.

Model equation (1) has one unknown parameter k corresponding to the coefficient of the bottom friction. The modeling was performed both at zero bottom friction ($k = 0$) and with account for the friction when the value of the coefficient was $k = 0.0006$. The value of this coefficient for long surface waves and internal waves was partly discussed in [5, 6, 26]). The geographical latitude of the section was taken the same for all points (41°5′ N). The results of wave-train modeling at points 15 and 16 are presented in Figs. 4 and 5. The displacement of the isopycnals at the point of maximum of the first linear mode obtained as a result of the numerical calculation (solid line) is shown in comparison with the displacement of the same isopycnals (dotted curve) plotted from the data of observations.

It follows from a comparison of the curves shown in Figs. 4 and 5 that, first, our model in both cases satis-

factorily describes the two first solitary waves and then a significant phase distortion of the solitary waves occurs.

Second, it is worth noting that the predicted form, amplitude, and location of the first two solitary waves is much closer to the observed ones when the bottom friction with a coefficient of $k = 0.0006$ is introduced in the model.

CONCLUSIONS

A comparison of the modeling results for an internal wave train with data from field observations demonstrated a significant influence of empirically introduced bottom friction on the amplitude and phase of internal waves. It was shown that, if the coefficient of bottom friction is 0.0006, the first two solitary waves are well described by the suggested model at distances of 13.5 km and 26 km from the point of the initial observation of the internal wave train. The description of the next peaks by the model both in regards to amplitude and phase is much worse. A similar good description of two first solitary waves was also obtained in the modeling of internal wave dynamics over the Malin shelf [18] It is worth noting that the following modeled solitary waves exceed the observed ones in regards to amplitude; additional peaks also appear in the experimental records. This is a typical situation that appeared in the modeling of the dynamics of the internal wave packet over the Malin shelf. Mismatched amplitudes can be caused by the fact that the first intense solitary waves lead to the partial mixing of the stratified fluid and variation in the mean stratification profile; hence, this causes errors in the recalculation of temperature measurements to the displacement of isopycnals. The appearance of additional peaks in the field record of internal wave train can be a sequence of wave refraction over bottom inhomogeneities, which is not taken into account in the one-dimensional version of the model. It is also possible that for the sake of better modeling it is worth taking into account the data of currents in the region of measurements. Nevertheless, a good reproduction of two first internal waves by the applied model can be considered the main result of this work and an indicator of the working capacity of the model for describing the internal wave transformation.

ACKNOWLEDGMENTS

The results presented here were obtained within the Federal Target Program "Scientific and Scientific–Pedagogical Personnel for an Innovative Russia, 2009–2013" (no. 14.B37.21.0611), the Russian Foundation for Basic Research (project nos. 12-05-00472, 13-05-90424_Ukr_f_a, 13-05-97037_R_Povolzhie), and Project of the NIU BSE Scientific Foundation no. 12-01-0103.

REFERENCES

1. Yu. Z. Miropol'skii, *Dynamics of Internal Gravity Waves in the Ocean* (Gidrometeoizdat, Leningrad, 1981).
2. E. N. Pelinovsky and S. Kh. Shavratsky, "Nonlinear wave propagation in an inhomogeneous ocean," Izv. Akad. Nauk, Fiz. Atmos. Okeana **12** (1), 86–92 (1976).
3. T. Kakutani and N. Yamasaki, "Solitary waves on a two-layer fluid," J. Phys. Soc. Jpn. **45**, 674–679 (1978).
4. C. Knickerbocker, "Internal solitary waves near a turning point," Phys. Lett. A **75**, 326–330 (1980).
5. P. E. Holloway, E. Pelinovsky, T. Talipova, and B. Barnes, "A nonlinear model of internal tide transformation on the Australian North-West Shelf," J. Phys. Oceanogr. **27** (6), 871–896 (1997).
6. P. Holloway, E. Pelinovsky, and T. Talipova, "A generalized Korteweg–De Vries model of internal tide transformation in the coastal zone," J. Geophys. Res. **104** (C8), 18333–18350 (1999).
7. A. Liu, J. Holbrook, and J. Apel, "Nonlinear internal wave evolution in the Sulu Sea," J. Phys. Oceanogr. **15**, 1613–1624 (1985).
8. A. K. Liu, Y. S. Chang, M.-K. Hsu, and N. K. Liang, "Evolution of nonlinear internal waves in the East and South China Seas," J. Geophys. Res. **103**, 7995–8008 (1998).
9. M. H. Orr and P. C. Mignerey, "Nonlinear internal waves in the South China Sea: Observation of the conversion of depression internal waves to elevation internal waves," J. Geophys. Res. **108** (C3), 3064 (2003).
10. W. Choi and R. Camassa, "Fully nonlinear internal waves in a two-fluid system," J. Fluid Mech. **396**, 1–36 (1999).
11. K. G. Lamb and L. Yan, "The evolution of internal wave undular bores: Comparisons of a fully nonlinear numerical model with weakly nonlinear theories," J. Phys. Oceanogr. **26** (12), 2712–2734 (1996).
12. V. Maderich, T. Talipova, R. Grimshaw, E. Pelinovsky, B. H. Choi, I. Brovchenko, and K. Terletska, "Interaction of a large amplitude interfacial solitary wave of depression with a bottom step," Phys. Fluids **22**, 076602 (2010).
13. V. Vlasenko and N. Stashchuk, "Three-dimensional shoaling of large-amplitude internal waves," J. Geophys. Res. **112**, C11018 (2007).
14. K. Lamb, O. Polukhina, T. Talipova, E. Pelinovsky, W. Xiao, and A. Kurkin, "Breather generation in the fully nonlinear models of a stratified fluid," Phys. Rev. E **75** (4), 046306 (2007).
15. R. Grimshaw, E. Pelinovsky, T. Talipova, and A. Kurkin, "Simulation of the transformation of internal solitary waves on oceanic shelves," J. Phys. Oceanogr. **34**, 2774–2791 (2004).

16. R. Grimshaw, E. Pelinovsky, and T. Talipova, "Modeling internal solitary waves in the coastal ocean," Surv. Geophys. **28** (2), 273–298 (2007).

17. E. N. Pelinovsky, N. V. Polukhin, and T. G. Talipova, "Modeling of the internal wave field characteristics in the Arctic," in *Surface and Internal Waves in Arctic Seas* (Gidrometeoizdat, St. Petersburg, 2002), pp. 235–237 [in Russian].

18. T. G. Talipova and E. N. Pelinovsky, "Modeling of the propagation of long internal waves in an inhomogeneous ocean: Theory and verification," Fundam. Prikl. Gidrofiz. **6** (2), 46–54 (2013).

19. D. R. G. Jeans and T. J. Sherwin, "The variability of strongly non-linear solitary internal waves observed during an upwelling season on the Portuguese shelf," Cont. Shelf Res. **21**, 1855–1878 (2001).

20. T. J. Sherwin, V. I. Vlasenko, N. Stashchuk, and D. R. G. Jeans, and B. Jones, "Along-slope generation as an explanation for some unusually large internal tides," Deep-Sea Res., Part I **49** (10), 1787–1799 (2002).

21. J. Small, "Internal tide transformation across a continental slope off Cape Sines Portugal," J. Mar. Syst. **32**, 43–69 (2002).

22. P. Holloway, E. Pelinovsky, and T. Talipova, "Internal tide transformation and oceanic internal solitary waves," in *Environmental Stratified Flows,* Ed. by R. Grimshaw (Kluwer Acad., 2001), Chap. 2, pp. 29–60.

Translated by E. Morozov